Journal of Alloys and Compounds, 191 (1993) 279–285
JALCOM 525

Hydrogenation and nitrogenation of $SmFe_3$

Chris N. Christodoulou and Takuo Takeshita
Central Research Institute, Mitsubishi Materials Corporation, 1-297 Kitabukuro-cho, Omiya, Saitama 330 (Japan)

(Received September 7, 1992)

Abstract

The characteristics of the reactions between $SmFe_3$ and H_2 or N_2 were studied by isochorothermal analysis, X-ray diffraction and thermomagnetic analysis. $SmFe_3$ absorbs about 3.1 atoms of hydrogen instantaneously at a temperature between 140 and 170 °C. Subsequent cooling to room temperature causes an increase in the hydrogen concentration to about 4 hydrogen atoms per mole of $SmFe_3$. As the temperature is increased, the $SmFe_3$ hydride begins to desorb hydrogen and its composition becomes $SmFe_3H_{0.2}$ at about 350 °C. The $SmFe_3$ hydride desorbs and absorbs hydrogen reversibly in the temperature range 25–400 °C, with a 16 °C temperature hysteresis occurring between 249 and 233 °C during heating and cooling. At about 425 °C, the hydride begins to decompose into Sm hydride and α-Fe. The decomposition reaction is accompanied by a massive hydrogen absorption. The $SmFe_3$ hydride has the rhombohedral crystal structure (same as the parent compound) with a 19% expanded lattice with parameters $a = 5.378$ Å and $c = 27.345$ Å. The stresses introduced by the huge lattice expansion cause the decrepitation of the $SmFe_3$ hydride samples. The Curie temperature and saturation magnetization are 90 °C and 70.8 e.m.u. g^{-1} for $SmFe_3H_4$ compared with 390 °C and 80.6 e.m.u. g^{-1} for $SmFe_3$. For both $SmFe_3$ and $SmFe_3$ hydride, the easy direction of magnetization is along the crystallographic c axis. $SmFe_3$ powder reacts with N_2 at about 250 °C forming SmN, α-Sm and α-Fe. The final products are SmN and α-Fe. No interstitial $SmFe_3$ nitride exists at any temperature.

1. Introduction

The RT_3 (where $R \equiv$ rare earth, $T \equiv$ Fe or Co) intermetallic compounds are known to exhibit a rhombohedral $PuNi_3$-type crystal structure [1]. They are also known to absorb appreciable amounts of hydrogen [2–5] forming interstitial RT_3 hydrides retaining their original crystal structure. The maximum solubility of hydrogen in the RCo_3 ($R \equiv$ Dy, Ho, Er) compounds was reported by Takeshita *et al.* [2] to be 5 H atoms per mole of RCo_3. The crystal structure and pressure–composition isotherms for the RT_3 hydrides ($R \equiv$ Gd, Td, Dy, Ho, Er and $T \equiv$ Fe, Co) have been studied by Bechman *et al.* [3]. In addition, Malik *et al.* [4–6] studied the effect of absorbed hydrogen on the magnetic properties of RT_3 ($R \equiv$ Gd, Dy, Ho and $T \equiv$ Fe, Co) and RFe_3 ($R \equiv$ Tb, Er and Tm). In general, the RT_3 compounds were found to absorb between 3 (*i.e.* $DyFe_3H_3$) and 5 (*i.e.* $ErCo_3H_5$) H atoms per mole of RT_3. The original lattice was found to expand by between 13% and 23% depending on the compound and the hydrogen concentration. In the case of RCo_3 ($R \equiv$ Gd, Dy and Ho), hydrogen absorption causes a reduction in the Co moment resulting in an increase in the total magnetization because of the antiparallel magnetic coupling between the rare earth and Co sublattices. In the case of RFe_3 ($R \equiv$ Gd, Dy and Ho), hydrogen absorption causes an increase in the Fe moment resulting in a decrease in the total magnetization. Hydrogen absorption was found to cause a large decrease in the Curie temperatures in the case of RCo_3 ($R \equiv$ Gd, Dy and Ho). In the case of the RFe_3 hydrides ($R \equiv$ Gd, Dy and Ho), the Curie temperatures are above room temperature, but could not be determined because the compounds desorb hydrogen below the Curie temperature.

So far attention has been focused mostly on the R(Co, Fe)$_3$ hydrides which contain heavy (Gd or heavier) rather than light rare earth elements. This is because they are expected to exhibit high equilibrium hydrogen pressures (higher than 1 atm) and could be useful as hydrogen storage materials [2]. Among the R(Co, Fe)$_3$ ($R \equiv$ light rare earth) compounds, only the YFe_3 hydride [7], YCo_3 hydride [8] and $CeCo_3$ hydride [9] have been studied. The only study concerning the $SmFe_3$ hydride, which is the focus of the present work was reported by Kost *et al.* [10]. No nitrogenation study on $SmFe_3$ has been reported in the literature.

The discovery of a new magnetic material, Sm_2Fe_{17} nitride [11] has triggered a renewed interest in the Sm–Fe intermetallic compounds in general. Permanent magnets have already been prepared on the Sm_2Fe_{17}

0925-8388/93/$6.00

nitride by several methods such as mechanical alloying (MA) [12, 13], rapid solidification [14, 15], conventional powder metallurgy [13, 16, 17] and hydrogen treatment (HDDR) [18, 19]. All of these methods involve two major steps: (a) the formation of the Sm_2Fe_{17} phase (preferably in a microcrystalline form) and (b) the nitrogenation of Sm_2Fe_{17} in N_2 or ammonia to form the interstitial Sm_2Fe_{17} nitride which exhibits hard magnetic properties.

Many studies have been published on the Sm_2Fe_{17} nitrides mainly concerning the nitrogenation kinetics [20, 21] and substitutions [11, 22–27] of Sm or Fe with other rare earth or transition metals respectively. In step (a) of the preparation method, one usually has to deal not only with the major Sm_2Fe_{17} phase but also with other phases such as Sm, $SmFe_2$, $SmFe_3$ and α-Fe. Consequently, during the whole process (steps (a) and (b)) one has to consider the reaction products of these "secondary" phases with hydrogen and nitrogen. The reaction products have an effect on the details of the processes as well as on the magnetic properties of the final product. Experience obtained when working with other magnetic materials, such as the $Nd_2Fe_{14}B$-based magnets, shows that the presence of the secondary phases plays an important role in the development of the intrinsic coercivity. At present, there is not adequate specific information on the kinetics and reaction products between the Sm–Fe alloys and hydrogen or nitrogen.

This lack of information has led us to make a series of studies on the reactions between Sm [28], $SmFe_2$ [29], $SmFe_3$ and Sm_2Fe_{17} single phases and hydrogen or nitrogen gas as a function of temperature. In the present study, the characteristics of the reactions between $SmFe_3$ and H_2 or N_2 are reported. The reactions of H_2 and N_2 with the Sm_2Fe_{17} phase will be reported in the near future. Such information on the reactions between the Sm–Fe alloys and H_2 or N_2 has been used to interpret the resulting phases and magnetic properties of the Sm_2Fe_{17} nitride-based permanent magnets prepared in our laboratory by several methods, which will also be published in the near future.

2. Experimental details

The $SmFe_3$ alloy was prepared by arc melting of the constituent elements (purity, better than 99.9 wt.%) in a pure argon gas atmosphere. During melting, 5 wt.% Sm excess was added to account for the Sm loss due to vaporization. The as-prepared $SmFe_3$ alloy was heat treated at 850 °C for about 1 week in order to produce an $SmFe_3$ single-phase alloy. The purity of H_2 and N_2 gases used for hydrogenation and nitrogenation was higher than 99.999 vol.%.

The constant volume reactor (isochorothermal analyser or ITA) which was used in the present study is similar to the thermopiezic analyser (TPA) used by other researchers (for instance, Coey *et al.* [11]) for the study of gas–solid reactions. The volume of the ITA was about 2.3 cm^3 and only about 5% of the total volume was heated. The $SmFe_3$ samples, weighing between 2 and 10 mg, were placed in a quartz tube (ITA) and heated with a precisely controlled programmable furnace capable of reaching a temperature of 1000 °C. The pressure was measured with a pressure sensor capable of detecting pressure differences of about 100 Pa. The temperature was measured with an accuracy of ± 1 °C. The pressure *vs.* temperature data were collected in a computer and analysed by taking into consideration the pressure variations due to the thermal effects (heated volume). By utilizing the ideal gas law, the data were transformed and plotted in terms of atoms of gas absorbed by the solid or desorbed from the solid as a function of temperature. The ideal gas law was considered to be a good approximation because of the relatively low pressure and high temperature conditions (0–125 kPa and 20–1000 °C) applied during the experiments. ITA isochores were obtained for the "$SmFe_3+H_2$" and "$SmFe_3+N_2$" systems in the temperature range 20–950 °C.

Phase analysis was performed by thermomagnetic analysis (TMA) and powder X-ray diffraction (XRD). Magnetization experiments were performed with a vibrating sample magnetometer (VSM) at 25 °C in a maximum applied field of 15 kOe. TMA was performed with a Faraday balance in the temperature range 25–900 °C and a magnetic field of about 1 kOe. The samples used in the Faraday balance were sealed in a quartz tube of known volume under argon or hydrogen gas, depending on the scope of the experiment. Powder XRD patterns were obtained under ambient conditions using a Philips automated diffractometer with Cu Kα radiation monochromated by a graphite single crystal. XRD patterns were obtained for both random powder and magnetically aligned powder which was fixed in epoxy resin.

3. Results and discussion

3.1. *Crystal structure and magnetic properties of $SmFe_3$*

The XRD pattern of the $SmFe_3$ alloy used in the present study is shown in Fig. 1. The alloy contains only the $SmFe_3$ phase which crystallizes in the rhombohedral $PuNi_3$-type structure and has lattice parameters of $a=5.180$ Å and $c=24.789$ Å. The absence of other phases, especially the Sm_2Fe_{17} phase, is confirmed by the XRD pattern of the aligned powder (Fig. 1(b)), which does not show any c-plane Bragg peaks (*i.e.*

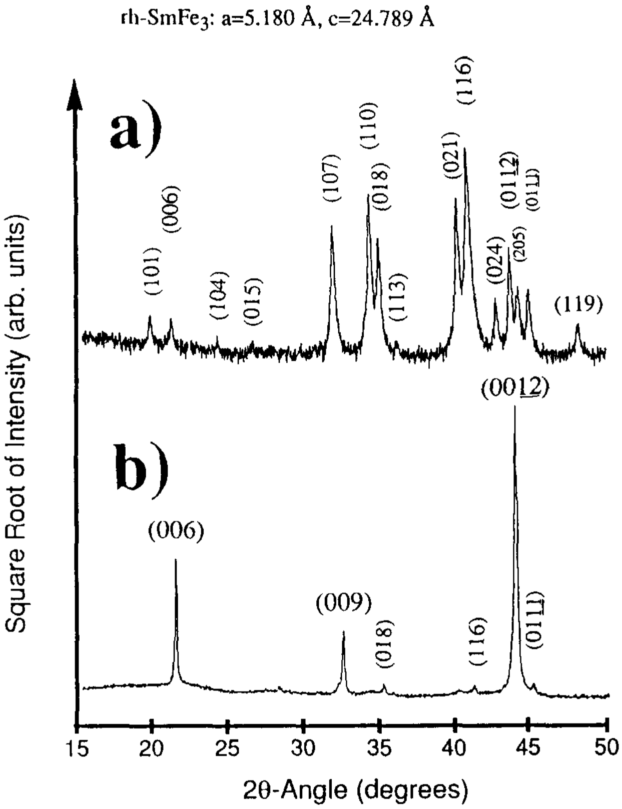

Fig. 1. XRD pattern of the $SmFe_3$ alloy: (a) Random powder; (b) Powder aligned in a magnetic field of 20 kOe and fixed in epoxy resin.

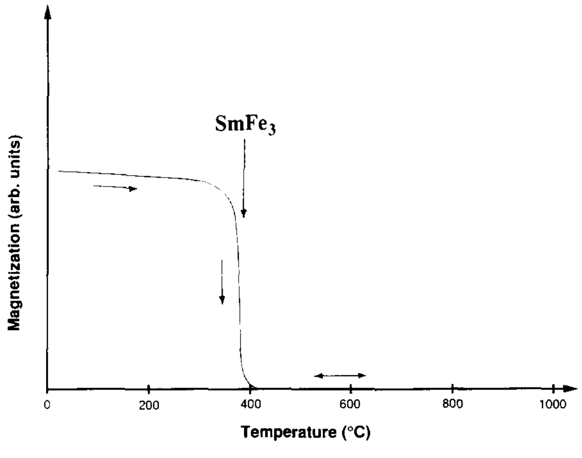

Fig. 2. TMA trace of the $SmFe_3$ alloy.

(110), (300) or (220)); these should be observed even if a small amount of the magnetically planar Sm_2Fe_{17} phase is present. In the same pattern, there is a large increase in the intensities of the (006), (009) and $(00\underline{12})$ Bragg peaks of the $SmFe_3$ phase. This is expected because the easy direction of magnetization (EDOM) is along the *c* axis [30]. The Curie temperature (T_c) of the $SmFe_3$ phase is 390 °C as shown in the TMA trace in Fig. 2. The TMA trace in Fig. 2 also confirms that the alloy does not contain other ferromagnetic phases (α-Fe with $T_c = 770$ °C, Sm_2Fe_{17} with $T_c = 135$ °C or $SmFe_2$ with $T_c = 410$ °C), except the $SmFe_3$ phase ($T_c = 390$ °C). The saturation magnetization (M_s) of the $SmFe_3$ phase (aligned powder) was measured by the VSM to be 80.6 e.m.u. g^{-1} in the maximum available field of 15 kOe.

3.2. *Reaction of $SmFe_3$ with hydrogen*

3.2.1. *Hydrogen absorption*

3.2.1.1. Isochorothermal analysis. Figure 3(a) shows the ITA isochore trace for the "$SmFe_3 + H_2$" system obtained under an initial hydrogen gas pressure of 122.29 kPa and an H to $SmFe_3$ ratio of 7.88. On heating, $SmFe_3H_{3.1}$ ($P_{H_2} = 110.23$ kPa) is formed instantly at a temperature of 170 °C. Subsequent cooling causes fur-

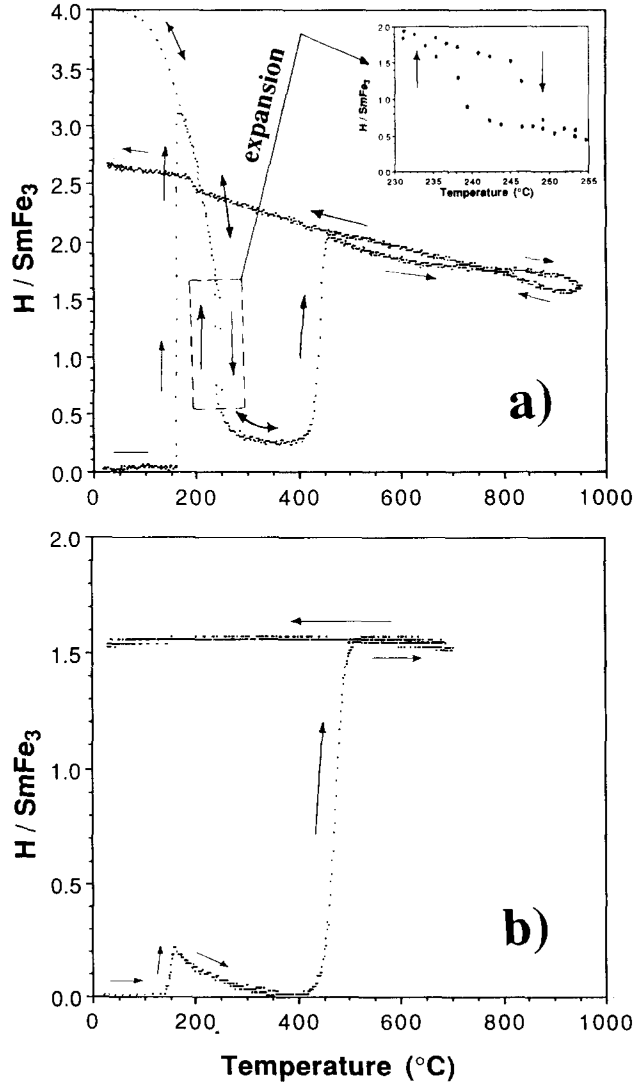

Fig. 3. ITA traces for the "$SmFe_3 + H_2$" system under different initial hydrogen gas pressures (P_0) and initial ratios of hydrogen gas atoms per mole of $SmFe_3$ (H/$SmFe_3$): (a) $P_0 = 122.29$ kPa, H/$SmFe_3 = 7.88$, $m = 2.78$ mg; (b) $P_0 = 12.70$ kPa, H/$SmFe_3 = 1.56$, $m = 4.83$ mg.

ther absorption and the hydrogen concentration reaches the value of 4 H atoms per $SmFe_3$. As the temperature is increased and immediately after its formation, $SmFe_3H_{3.1}$ begins to desorb hydrogen gradually, with a sharp decrease in the hydrogen content from 1.5 to 0.6 H atom per $SmFe_3$ occurring between the temperatures of 244 and 249 °C. Further heating causes an additional small decrease in the hydrogen content to the level of 0.2 H atom per $SmFe_3$. This hydrogen content remains almost constant up to a temperature of 425 °C where a massive hydrogen absorption occurs with the $SmFe_3$ hydride decomposing into Sm hydride and α-Fe according to the reaction

$$SmFe_3H_\delta + H_2 = \text{Sm hydride} + \alpha\text{-Fe}$$

where $\delta \approx 0.2$. On cooling to room temperature, α-Fe remains unaffected but the Sm hydride absorbs more hydrogen at about 190 °C resulting in an Sm hydride of composition $SmH_{2.53}$. This feature of the ITA trace is very common for the Sm hydrides as observed in a study of the reaction between Sm metal and hydrogen gas [28].

Temperature cycling experiments performed with the ITA for the "$SmFe_3H_4 + H_2$" system showed that hydrogen desorption and absorption are completely reversible between the temperatures of 25 and 400 °C with a temperature hysteresis of 16 °C occurring between 249 and 233 °C between heating and cooling (Fig. 3(a)). The sharp decrease (on heating) and increase (on cooling) of the hydrogen concentration (of about 1 H atom per $SmFe_3$) is believed to be due to a preferential occupation or evacuation of certain interstitial sites of the rhombohedral structure by hydrogen atoms.

Figure 3(b) shows the ITA trace for the "$SmFe_3 + H_2$" system obtained under an initial hydrogen gas pressure of 12.70 kPa and an H to $SmFe_3$ ratio of 1.56. Hydrogen absorption begins at 140 °C and the hydrogen concentration reaches its highest value of 0.21 H atom per $SmFe_3$ ($P_{H_2} = 8.25$ kPa) at 156 °C. The low-hydrogen-concentration $SmFe_3$ hydride is a result of the low hydrogen gas pressure applied during the experiment as expected in gas–solid reactions. As the temperature is increased, the hydride begins to desorb hydrogen gradually reaching a near-zero concentration at 337 °C, followed by a massive hydrogen absorption at about 425 °C as a result of the decomposition of $SmFe_3$ into α-Fe, Sm hydride and Sm. During decomposition, all of the available hydrogen is absorbed and the entire amount of $SmFe_3$ is decomposed in contrast with the $SmFe_2$ compound [29] where some $SmFe_2$ remains unaffected. This is attributed to the fact that the reaction of hydrogen with $SmFe_3$ occurs homogeneously, whereas $SmFe_2$ reacts with hydrogen rather locally. The presence of elemental Sm (shown later in Section 3.2.1.2) is the result of the complete decomposition of $SmFe_3$ and the lack of enough hydrogen to react with it; one mole of Sm "needs" two hydrogen atoms to form SmH_2, but only 1.33 are available during the ITA experiment (Fig. 3(b)).

3.2.1.2. X-ray diffraction. Figure 4 shows the XRD pattern for the $SmFe_3H_4$ powder. It exhibits the rhombohedral crystal structure with lattice parameters of $a = 5.378$ Å and $c = 27.345$ Å compared with those of $a = 5.180$ Å and $c = 24.789$ Å of the original $SmFe_3$ phase (Fig. 1(a)). This corresponds to a 19% lattice expansion. The stresses introduced in the $SmFe_3$ hydride sample cause its decrepitation resulting in a fine powder of $SmFe_3$ hydride. The XRD pattern for the aligned powder (Fig. 4(d)) suggests that, at room temperature, $SmFe_3H_4$ exhibits a uniaxial magnetocrystalline anisotropy. The EDOM is along the crystallographic c axis.

Figure 5 shows the XRD pattern of the sample at the end of the ITA experiment shown in Fig. 3(b). The sample contains α-Fe, Sm dihydride and some poorly crystallized elemental Sm, evident by the presence of the f.c.c.-SmO [28]. In the sample at the end of the ITA experiment shown in Fig. 3(a), no traces of Sm were found since hydrogen was readily available to react with the entire amount of Sm forming Sm hydride.

3.2.1.3. Thermomagnetic analysis – magnetization measurements. Figure 6 shows the TMA trace of an $SmFe_3H_4$ sample which was sealed in a small quartz tube under approximately 0.9 atm argon gas atmosphere. The Curie

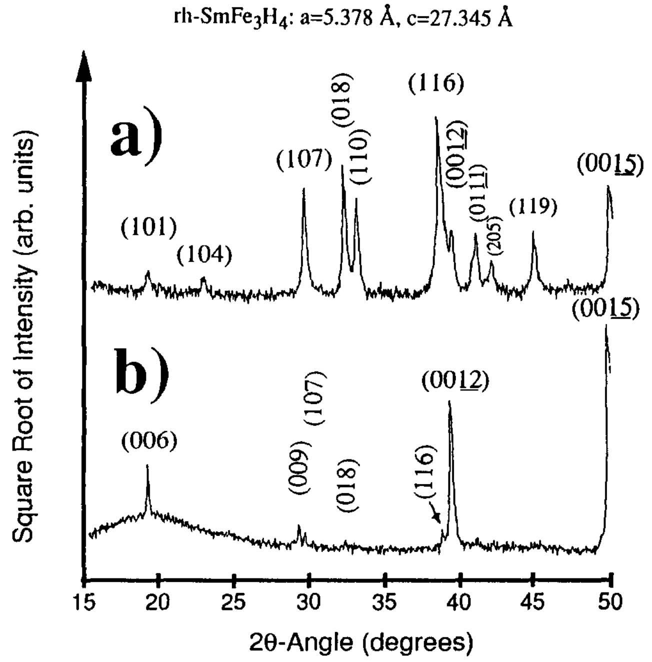

Fig. 4. XRD pattern of $SmFe_3H_4$: (a) random powder; (b) powder aligned in a magnetic field of 20 kOe and fixed in epoxy resin.

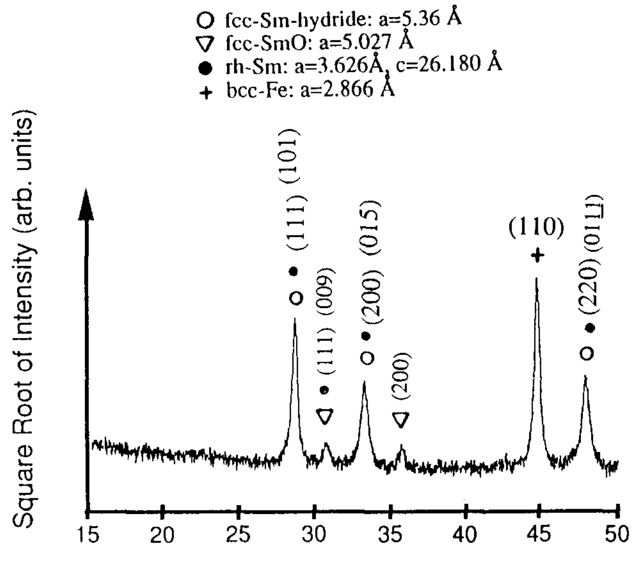

Fig. 5. XRD pattern of the sample at the end of the ITA trace shown in Fig. 3(b).

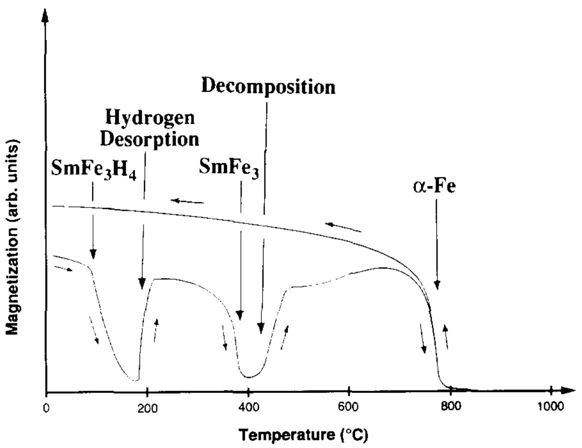

Fig. 6. TMA trace of an SmFe$_3$H$_4$ sample which was sealed in a small quartz tube under approximately 0.9 atm argon gas atmosphere.

temperature of the hydride is about 90 °C. At about 180 °C, there is a sharp increase in the magnetization due to the desorption of hydrogen and the formation of SmFe$_3$ (or a low-hydrogen-concentration SmFe$_3$) for which the Curie temperature is about 390 °C as shown in the same TMA trace. At about 425 °C, the magnetization of the sample increases again because SmFe$_3$ decomposes into α-Fe and Sm hydride. The cooling part of the TMA trace suggests that the decomposition products are only α-Fe ($T_c = 770$ °C) and Sm hydride.

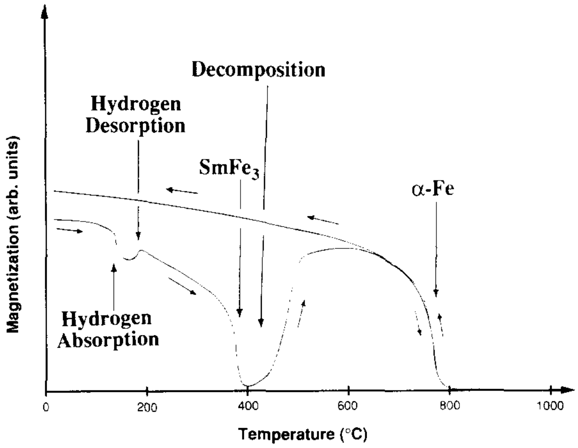

Fig. 7. TMA trace of an SmFe$_3$ sample which was sealed in a small quartz tube under approximately 0.7 atm hydrogen gas atmosphere.

Figure 7 shows the TMA trace of an SmFe$_3$ sample which was sealed in a small quartz tube under approximately 0.7 atm hydrogen gas atmosphere. The initial H atom to SmFe$_3$ ratio was about 5.0. On heating, SmFe$_3$ absorbs hydrogen at about 150 °C and the magnetization of the sample decreases since the T_c value of SmFe$_3$ hydride is about 90 °C, as has been shown previously. Further heating causes hydrogen desorption regenerating SmFe$_3$ and the magnetization of the sample increases. Above 425 °C, the magnetization increases due to the decomposition of SmFe$_3$ into α-Fe and Sm hydride which remain the same after cooling to room temperature.

The saturation magnetization (at 15 kOe, 25 °C) for SmFe$_3$H$_4$ was measured with a VSM and found to be 70.8 e.m.u. g^{-1} compared with 80.6 e.m.u. g^{-1} for SmFe$_3$. A similar decrease in the saturation magnetization has been observed [5, 6] to occur in the RFe$_3$-hydrides (R$\equiv$Gd or heavier rare earth) and is due to the increase in the Fe sublattice moment resulting in a decrease in the total magnetization (antiparallel coupling). In the case of the RFe$_3$ hydrides with R$\equiv$ light rare earth, the magnetization is expected to increase because of the parallel coupling between the Fe and R sublattice moments.

3.2.1.4. Decomposition reaction mechanism. Possible decomposition mechanisms which explain the coexistence of α-Fe, Sm hydride and elemental Sm are as follows. Initially, hydrogen causes the decomposition of SmFe$_3$ into Sm + α-Fe and then it reacts readily with Sm to form Sm hydride. If the amount of hydrogen is limited (H/SmFe$_3$ < 2), then some of the Sm will remain. In the case where hydrogen is readily available, the entire amount of Sm will react forming stable Sm hydride. It is also possible that, just before decomposition, a metastable SmFe$_3$ hydride is formed which decomposes instantly into α-Fe, Sm hydride and Sm (if its hydrogen concentration is below 2H atoms per mole of SmFe$_3$). The existence of a metastable SmFe$_3$ hydride is supported by the fact that, even in the presence of a limited amount of hydrogen (H/SmFe$_3$ < 2), the entire amount of SmFe$_3$ decomposes.

Nevertheless, no direct experimental evidence of the presence of such a metastable $SmFe_3$ hydride has been observed.

3.2.2. Hydrogen desorption

Figure 8 shows the ITA isochore trace for $SmFe_3H_{3.4}$ under initial vacuum conditions. Hydrogen desorption begins at 150 °C and is complete at 210 °C. The highest desorption rate occurs at about 180 °C in accordance with the observations in the TMA trace shown in Fig. 6. Between the temperatures of 210 and 400 °C, the interstitial hydrogen concentration remains essentially constant at 0.2 H atom per $SmFe_3$. This is followed by a massive hydrogen absorption at about 425 °C due to the decomposition of $SmFe_3$ into α-Fe and Sm hydride, exactly as observed previously (see Figs. 3(a) and 6).

3.3. Reaction of $SmFe_3$ with nitrogen

The ITA traces for powder and bulk $SmFe_3$ in a nitrogen atmosphere are shown in Fig. 9. The powder sample begins to react with nitrogen at about 250 °C compared with 450 °C in the case of the bulk sample. The reaction seems to be complete at about 600 °C and 950 °C for the powder and bulk samples respectively. The XRD patterns of the $SmFe_3$ powder samples heat treated under nitrogen gas at 450 and 950 °C are shown in Fig. 10. At 450 °C, $SmFe_3$ coexists with SmN, α-Fe and elemental Sm. At 950 °C, the reaction is complete and only SmN and α-Fe exist. The nitrogenation of $SmFe_3$ seems to occur in a similar manner to that of $SmFe_2$. In the case of the nitrogenation of $SmFe_2$, it has been suggested [29] that nitrogen initially causes the decomposition of the compound into α-Fe and Sm with subsequent reaction of nitrogen with Sm to produce SmN. The nitrogenation mechanism seems to be the same for both $SmFe_3$ and $SmFe_2$ since elemental Sm was also formed during the nitrogenation of $SmFe_3$. As with $SmFe_2$, no interstitial $SmFe_3$ nitride was found to exist.

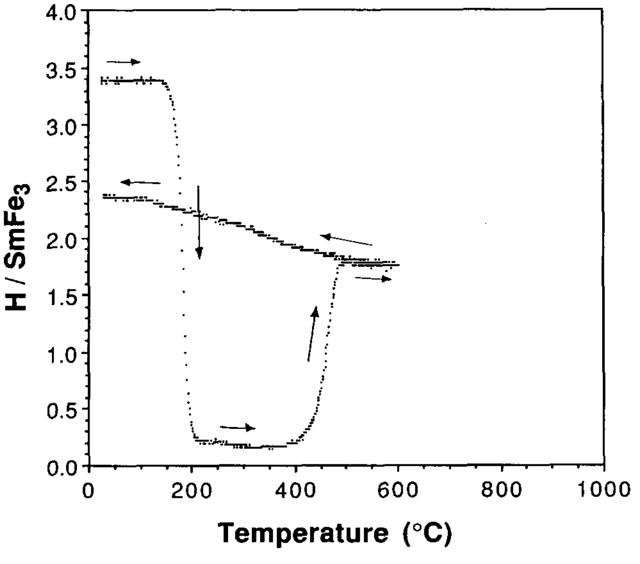

Fig. 8. ITA trace for $SmFe_3H_{3.4}$ (m = 2.61 mg) under initial vacuum conditions.

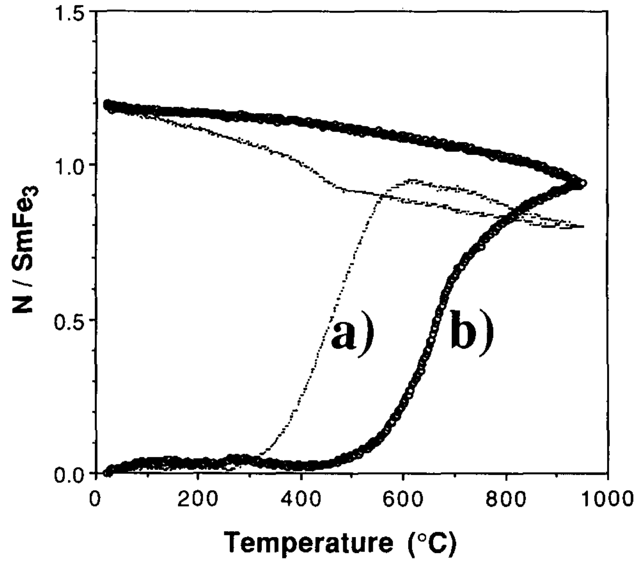

Fig. 9. ITA trace for the "$SmFe_3+N_2$" system: (a) powder sample, P_0 = 116.67 kPa, N/$SmFe_3$ = 4.36, m = 8.25 mg; (b) bulk sample, P_0 = 117.67 kPa, N/$SmFe_3$ = 3.78, m = 9.62 mg.

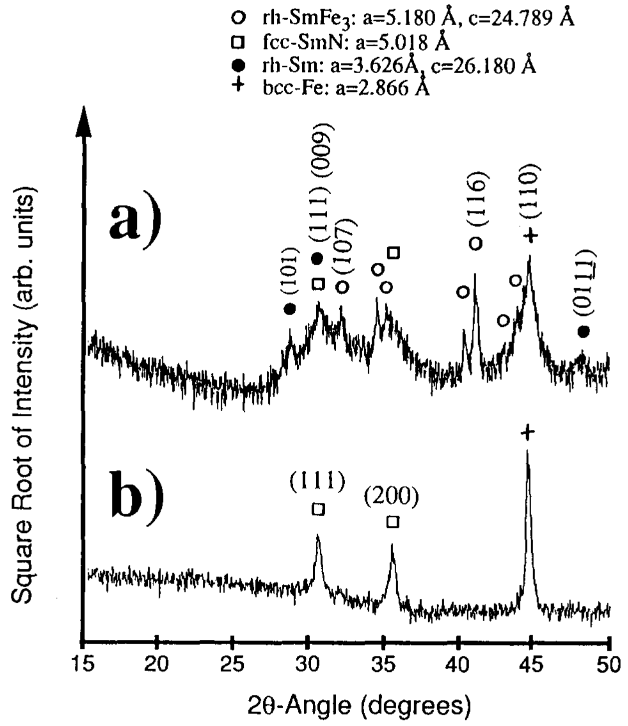

Fig. 10. XRD patterns of the $SmFe_3$ powder samples heat treated under nitrogen gas at the temperature of 450 °C (a) and 950 °C (b).

4. Conclusions

By heating $SmFe_3$ under relatively low pressures (10–125 kPa) of hydrogen gas, hydrogen is readily absorbed at about 140–170 °C forming an interstitial $SmFe_3$ hydride with a room temperature composition of $SmFe_3H_4$. Both $SmFe_3$ and $SmFe_3H_4$ have the same rhombohedral crystal structure and an EDOM along the c axis. The $SmFe_3H_4$ lattice is expanded 19% with respect to the $SmFe_3$ lattice and this induces the decrepitation of the samples forming a fine powder. Compared with $SmFe_3$, $SmFe_3H_4$ has a lower saturation magnetization (70.8 e.m.u. g^{-1} compared with 80.6 e.m.u. g^{-1}) and a lower Curie temperature (90 °C compared with 390 °C). On heating and immediately after its formation, the $SmFe_3$ hydride desorbs hydrogen gradually up to about 425 °C, where the low-hydrogen-concentration $SmFe_3$ hydride decomposes into α-Fe and Sm hydride. The decomposition is accompanied by a massive hydrogen absorption. A decomposition reaction mechanism has been suggested where hydrogen causes the initial decomposition of $SmFe_3$ into α-Fe and Sm, followed by a fast reaction between Sm and hydrogen forming Sm hydride.

Nitrogenation of $SmFe_3$ powder is initiated at about 250 °C forming SmN, α-Fe and Sm. The total reaction rate is controlled by the reaction rate between Sm and nitrogen which is fairly slow. The end products are α-Fe and SmN. No interstitial $SmFe_3$ nitride is formed at any temperature.

References

1 K. H. J. Buschow, *Phys. Status Solidi A, 7* (1971) 199.
2 T. Takeshita, W. E. Wallace and R. S. Graig, *Inorg. Chem., 13* (1974) 2283.
3 C. A. Bechman, A. Goudy, T. Takeshita, W. E. Wallace and R. S. Graig, *Inorg. Chem., 15* (1976) 2184.
4 S. K. Malik, W. E. Wallace and T. Takeshita, *Solid State Commun., 28* (1978) 977.
5 S. K. Malik, T. Takeshita and W. E. Wallace, *Magn. Lett., 1* (1976) 33.
6 S. K. Malik, F. Pourarian and W. E. Wallace, *J. Magn. Magn. Mater., 40* (1983) 27.
7 K. H. J. Buschow, *Solid State Commun., 19* (1976) 421.
8 M. Yamaguchi, M. Ikeda, H. Ohta, T. Katayama and T. Goto, *J. Less-Common Met., 106* (1985) 165.
9 R. H. Van Essen and K. H. J. Buschow, *J. Less-Common Met., 70* (1980) 189.
10 M. E. Kost, V. I. Mikheeva, M. V. Raevskaya, E. I. Yaropolova and A. L. Shilov, *Russ. J. Inorg. Chem., 24* (12) (1979) 1773.
11 J. M. D. Coey, H. Sun and Y. Otani, A new family of rare earth iron nitrides, in S. G. Sankar (ed.), *Proc. Sixth Int. Symp. on Magnetic Anisotropy and Coercivity in Rare Earth–Transition Metal Alloys,* Pittsburgh, PA, October 25, 1990, p. 36.
12 K. Schnitzke, L. Schultz, J. Wecker and M. Katter, *Appl. Phys. Lett., 57* (1990) 2853.
13 M. Endoh, M. Iwata and M. Tokunaga, *J. Appl. Phys., 70* (1991) 6030.
14 C. N. Christodoulou and T. Takeshita, Sm_2Fe_{17}-nitride-based permanent magnets produced by rapid solidification, *J. Alloys Comp.,* in press.
15 M. Katter, J. Wecker and L. Schultz, *J. Appl. Phys., 70* (1991) 3188.
16 J. M. D. Coey and H. Sun, *J. Magn. Magn. Mater., 87* (1990) L251.
17 M. Q. Huang, L. Y. Zhang, B. M. Ma, Y. Zheng, J. M. Elbicki, W. E. Wallace and S. G. Sankar, *J. Appl. Phys., 70* (1991) 6027.
18 C. N. Christodoulou and T. Takeshita, Sm_2Fe_{17}-nitride-based permanent magnets prepared by HDDR, *J. Alloys Comp.,* in press.
19 H. Nakamura, K. Kurihara, T. Tatsuki, S. Sugimoto, M. Okada and M. Homma, Variation of magnetic properties of $Sm_2Fe_{17}N_x$ alloys by hydrogen treatment, *Digests of the 15th Annual Conference on Magnetics in Japan, October 29–November 1, 1991,* Magnetic Society of Japan, Ibaraki, p. 379.
20 J. M. D. Coey, J. F. Lawler, H. Sun and J. E. Allan, *J. Appl. Phys., 69* (1991) 3007.
21 T. Mukai and T. Fujimoto, *J. Magn. Magn. Mater., 103* (1992) 165.
22 M. Q. Huang, B. M. Ma, W. E. Wallace and S. G. Sankar, Magnetic properties and structure of nitrogenated $R_2(Fe, Co)_{17}$ intermetallic compounds, in S. G. Sankar (ed.), *Proc. Sixth Int. Symp. on Magnetic Anisotropy and Coercivity in Rare Earth–Transition Metal Alloys, Pittsburgh, PA, October 25, 1990, p. 204.*
23 L. Y. Zhang, Y. Zheng and W. E. Wallace, Magnetization and PCI's of nitrogenated $R_2(Fe, Co)_{17}$ systems, in S. G. Sankar (ed.), *Proc. Sixth Int. Symp. on Magnetic Anisotropy and Coercivity in Rare Earth–Transition Metal Alloys, Pittsburgh, PA, October 25, 1990, p. 219.*
24 K. H. J. Buschow, R. Coehoorn, D. B. Mooij, K. de Waard and T. H. Jacobs, *J. Magn. Magn. Mater., 92* (1990) L35.
25 J. M. D. Coey, H. Sun and D. P. F. Hurley, *J. Magn. Magn. Mater., 101* (1991) 310.
26 M. Q. Huang, Y. Zheng, K. Miller, J. M. Elbicki and S. G. Sankar, *J. Appl. Phys., 70* (1991) 6024.
27 D. P. F. Hurley and J. M. D. Coey, *J. Magn. Magn. Mater., 99* (1991) 229.
28 C. N. Christodoulou and T. Takeshita, *J. Alloys Comp., 190* (1992) 99.
29 C. N. Christodoulou and T. Takeshita, *J. Alloys Comp.,* in press.
30 A. M. van der Kraan, J. N. J. van der Velden, J. H. F. van Apeldoorn, P. C. N. Gubbens and K. H. J. Buschow, *Phys. Status Solidi (A), 35* (1976) 137.